J Mol Neurosci
DOI 10.1007/s12031-014-0275-x

Protocadherin 11 X Regulates Differentiation and Proliferation of Neural Stem Cell In Vitro and In Vivo

Peng Zhang · Cuiying Wu · Ning Liu · Lijun Niu · Zhongjie Yan · Yanyan Feng · Ruxiang Xu

Received: 2 January 2014 / Accepted: 25 February 2014

Abstract Protocadherin 11 X-linked (Pcdh11x) protein is a member of the cadherin superfamily with established roles in cell adhesion. Previous studies have shown the molecular biology and possible relevance of Pcdh11x with neurological disease in humans. However, little is known about the neurophysiological function of Pcdh11x in neural development. Here, we verified that Pcdh11x is primarily expressed in various brain areas including the cortex, hippocampus, and ventricular/subventricular zone (VZ/SVZ) at different embryonic stages. Furthermore, both in vitro and in vivo experiments showed that Pcdh11x decreased neural differentiation but increased the neural proliferation. These observations demonstrate a crucial function for Pcdh11x during the development of central nervous system.

Keywords Protocadherin 11 X-linked protein · Neural stem cell · Differentiation · Proliferation · Migration

Introduction

The cadherin superfamily proteins are calcium-dependent adhesion glycoproteins that are critical for neural morphogenesis in the embryonic phase and for neural connections in the adult phase. The cadherin family includes classic cadherins, desmosomal cadherins, protocadherins (Pcdhs), and other proteins (Morishita and Yagi 2007). The members have fundamental roles in neural development, such as neurulation, dendritic morphogenesis, and axon pathfinding (Benson et al. 2001). Pcdhs are primarily expressed in the nervous system and are the largest subgroup of the cadherin superfamily. This superfamily includes 58 clustered and 13 nonclustered genes (Morishita and Yagi 2007).

Pcdh11x belongs to Pcdhs, which are transmembrane cell adhesion molecules expressed predominantly in the brain (Frank and Kemler 2002). Pcdh family can be divided into two groups based on their genomic structures: the clustered and nonclustered Pcdhs (Morishita and Yagi 2007). Clustered Pcdhs are classified into α, β, and γ subfamilies according to their clustered genetic organization (Wu and Maniatis 1999). An additional nonclustered group can be further classified based on the number of extracellular cadherin repeats (ECs) and features of the cytoplasmic domain, into Pcdh δ family, and other solitary Pcdhs (Morishita and Yagi 2007; Redies et al. 2005; Vanhalst et al. 2005). The Pcdh11 belongs to Pcdh δ family, including an ectodomain of seven ECs, a short transmembrane region, and a variable length cytoplasmic domain differing between isoforms (Priddle and Crow 2013). There are two types of Pcdh11, which were found in the homologous block of chromosomes X and Y: *pcdh11x* at Xq21.3 and *pcdh11y* at Yp11.2. Women express Pcdh11x, whereas men express both Pcdh11x and Pcdh11y (Priddle and Crow 2013). Transcriptional messenger RNA (mRNA) levels for both Pcdh11x and Pcdh11y have been detected in various brain regions, and both Pcdh11x and Pcdh11y regulate cell-cell adhesion rather than directly mediating adhesion (Kim et al. 2011). Other nonclustered Pcdhs, including Pcdh8 (arcadlin) and Pcdh10 (OL-Pcdh), have been studied in many contexts. For example, Pcdh8, which first appears at embryonic day 8.5 (E8.5), can regulate synaptic transmission

Peng Zhang and Cuiying Wu contribute equally to this work.

P. Zhang · R. Xu (✉)
Bayi Brain Hospital, Bayi Clinical Medical Institute, Southern Medical University, Beijing, China
e-mail: zjxuruxiang@163.com

P. Zhang · C. Wu · N. Liu · L. Niu · Z. Yan · Y. Feng · R. Xu
Bayi Brain Hospital, The Military General Hospital of Beijing PLA, No. 5 Nanmen CangDongcheng District Beijing 100700, China

Z. Yan
Department of Neurosurgery, the Second Hospital of Hebei Medical University, Shijiazhuang, China

Published online: 20 March 2014

and synaptic structure (Bozdagi et al. 2000; Tanaka et al. 2000; Yamagata et al. 1999). Pcdh10, which is primarily expressed in the olfactory bulb, limbic system, and cerebellum, is involved in synapse formation and cerebellum development (Benson et al. 2001; Bruses 2000; Hirano et al. 1999; Luckner et al. 2001; Redies 2000; Shapiro and Colman 1999; Yagi and Takeichi 2000). Some articles have demonstrated that Pcdh11x defects may cause sexual dimorphism and language delay (Lopes et al. 2006; Speevak and Farrell 2011); however, thus far, there have been few detailed studies about the neurophysiology roles of Pcdh11x. Pcdh11x belongs to the cadherin family; therefore, we considered whether Pcdh11x has a direct effect on cell-cell connections or not. Previous studies have indicated that Pcdhs have cell aggregation activity in a Ca^{2+}-dependent manner, which is similar to the classical cadherins, and showed that Pcdhs have homophilic interaction activity (Suzuki 1996).

Pcdh11x is predominantly expressed in the nervous tissue, suggesting that its primary function is in the brain. The aim of this study was to map the function of Pcdh11x in the nervous system. We found that Pcdh11x not only decreases the differentiation of neural stem cells to neurons and premature migration but also increases neural proliferation.

Experimental Procedures

Animals

CD1 (ICR) mice were purchased from the Vital River Company (Beijing, China). All surgical procedures were conducted according to the guidelines of the National Institutes of Health.

Neural Stem Cell Isolation and Culture

To collect neural stem cells, we extracted the whole brain from each mouse embryo at E13.5 and dissected irrelevant tissues away from the ventricular/subventricular zone (VZ/SVZ). Then, after washing the tissue using 0.01 M phosphate-buffered saline (PBS) containing penicillin-streptomycin (Invitrogen, Carlsbad, CA, 15140-122, 10,000 U/ml), we treated the VZ/SVZ tissues at 37 °C for 5 min. VZ/SVZ regions were then dissociated by gentle pipetting. Neural stem cells were cultured in medium containing DMEM/F12 (DMEM/F12 1:1 media, HyClone, SH3002301B), Neurobasal medium (Invitrogen, Carlsbad, CA, 21103-049), B-27® serum-free supplement (Invitrogen, Carlsbad, CA, 12587010, 2 %), N2 supplement (Invitrogen, Carlsbad, CA, 17502-048, 1 %), basic fibroblast growth factor (bFGF) (Sigma-Aldrich, Saint Louis, MO, SRP4037, 20 ng/ml), epidermal growth factor (EFG) (Sigma-Aldrich, Saint Louis, MO, SRP3027, 20 ng/ml), and L-glutamine (Invitrogen, Carlsbad, CA, 21051-024, 2 mM) in 25-cm^2 culture flasks. After 24 h, neural stem cell spheres appeared. We changed the culture medium every 2–3 days and passaged the cells when the diameter of spheres became larger than 100 μm (Barnabe-Heider et al. 2005; Hirabayashi et al. 2004).

In vitro Differentiation and Proliferation Assays

Plates were coated with poly-L-lysine hydrobromide (Sigma-Aldrich, Saint Louis, MO, P1399, 0.1 mg/ml) and laminin (Sigma-Aldrich, Saint Louis, MO, L2020, 1 μg/cm^2). For in vitro differentiation, neural stem cells (NSCs) were cultured in NSC medium, which was supplemented with fetal bovine serum (Invitrogen, Carlsbad, CA, 10099133, 1 %) without EGF and bFGF. After 5 days, cells were stained with Tuj-1 (anti-tubulin antibody, Chemicon-Millipore, MAB1637, 1:1,000). For proliferation, we seeded mouse embryonic neural stem cells at 5×10^5 cells per well in 24-well plates. After 24–48 h in culture, NSCs were incubated with 5-bromo-2′-deoxyuridine (BrdU; Sigma-Aldrich, Saint Louis, MO, B9285, 10 μM) at 37 °C with 5 % CO_2 for 1–2 h. Then, cells were stained with anti-BrdU antibody (Millipore, MAB3222, 1:1,000) overnight at 4 °C. Cells were then rinsed in 0.01 M PBS three times for 15 min followed by incubation in goat anti-mouse (Alexa Fluor® 488 goat anti-mouse IgG (H+L), Invitrogen, Carlsbad, CA, A-11001, 1:1,000) for 2 h at RT followed by washing three times for 15 min with PBS.

Tissue Preparation and Immunofluorescence

Mice were anesthetized using sodium phenobarbital. We collected tissues from different time points and fixed them with paraformaldehyde (Sigma-Aldrich, Saint Louis, MO, 158127, 4 %) in 0.1 M PBS, after dehydrating the tissues overnight in 0.1 M PBS with sucrose (Amresco, 57-50-1, 30 %). Tissues were stored at −80 °C until use. Frozen sections were cut 10 μm thick. Sections were stained with primary antibodies that were diluted in 0.1 M PBS with 10 % BSA overnight at 4 °C. The next day, sections were washed three times, each time for 5 min, in 0.01 M PBS at room temperature then incubated in secondary antibody for 1 h at 37 °C. Sections were then mounted using mounting medium with DAPI (Vectashield Mounting Medium with DAPI, Vector lab, H-1200). The following antibodies with corresponding dilutions were used for the studies: Pcdh11x (E-13), (Santa Cruz, sc-103726, 1:50), nestin (anti-nestin antibody, Millipore, MAB353, 1:800), Tuj-1 (anti-tubulin antibody, Chemicon-Millipore, MAB1637, 1:1,000), anti-glial fibrillary acidic protein (GFAP) (Cambridge, MA, ab7260, 1:1,000), NeuN (anti-NeuN antibody, Millipore, MAB377, 1:500), Sox-2 (SOX_2 rabbit monoclonal antibody, Burlingame, CA, Epitomics, 2683-1, 1:50), Ctip2 (anti-Ctip2 antibody, Abcam, Cambridge, MA, ab28448, 1:500), Tbr1 (anti-TBR1 antibody,

Abcam, Cambridge, MA, ab31940, 1:500), Tbr2 (anti-TBR2/eomes antibody, Abcam, Cambridge, MA, ab23345,1:500), Pax6 (mouse monoclonal [AD2.38] to PAX6, Abcam, Cambridge, MA, ab78545, 1:1,000), and Ki67 (rabbit polyclonal to Ki-67, Abcam, Cambridge, MA, ab15580, 1:250). The following Alexa Fluor-conjugated secondary antibodies were obtained from Invitrogen: Alexa Fluor® 488 rabbit anti-goat IgG (H+L), A11078; Alexa Fluor® 488 goat anti-mouse IgG (H+L), A-11001; Alexa Fluor® 594 rabbit anti-mouse IgG (H+L), A-11062; Alexa Fluor® 488 donkey anti-rat IgG (H+), A-21208. All antibodies were diluted 1:1,000 in blocking reagent.

Tissue Preparation and Immunohistochemistry

The brains were dissected from adult CD1 mice. The brains were fixed overnight in paraformaldehyde, transferred to an automatic dewatering machine (Leica, TP1020), and processed and embedded into paraffin. Sections were cut 5 μm thick for immunohistochemistry. Sections were blocked in PBS containing 10 % bovine serum albumin (BSA) and 0.3 % Triton X-100 (Sigma-Aldrich, Saint Louis, MO, T9284), then incubated with anti-Pcdh11x (E-13) (Pcdh11x (E-13), Santa Cruz, sc-103726, 1:50) or blocking peptide (Pcdh11x (E-13), Santa Cruz, sc-103726p) overnight at 4 °C. Afterward, sections were incubated with horseradish peroxidase (HRP) detection system (Polink-2 plus® polymer HRP detection system, for goat primary antibody, ZSGB, Beijing, PV-9003) for 30 min. DAB kit (ZSGB, Beijing, ZLI-9017) was used as the chromogen. Images were captured under a phase contrast microscope (Leica DM3000).

Plasmid Transfection and Immunofluorescence

Human embryonic kidney (HEK) 293T cells were cultured at 5×10^5/ml and were transfected with 1 μg *pCAG-pcdh11x-GFP* using the Lipofectamine™ 2000 transfection reagent (Invitrogen, Carlsbad, CA, 11668-019) according to company's instructions. After 48 h, cells were fixed as described above and treated with the Pcdh11x antibody.

RNA Isolation, Reverse Transcription, and Polymerase Chain Reaction

Total RNAs were isolated with TRIzol® reagent (Invitrogen, Carlsbad, CA, 15596018), and we used RNasin (TIANGEN, Beijing, DP418) to inhibit RNA degradation. Reverse transcription was performed using dNTP mixture (TIANGEN, Beijing, CD117), oligo (dT) (TIANGEN, Beijing, CD106), TIANScript MMLV (TIANGEN, Beijing, ER104), and DNase/RNase-free deionized water (TIANGEN, Beijing, RT121); then, the first-strand complementary DNAs (cDNAs) were collected.

The Primer 5 software was used to design primers from the conserved sequences of mus-pcdh11x. The primers which were targeted at a region common to all isoforms were the following: *pcdh11x-F* 5′-CTTTACAGCATTGTTGGAGGAA-3′ and *pcdh11x-R* 5′-GGTTGGCGGCATCTTACT-3′. The primers of *β-actin, nestin,* and *Sox-2* were the following: *β-actin-F* 5′-CCGAGCGTGGCTACAGCTTC-3′, *β-actin-R* 5′-ACCTGGCCGTCAGGCAGCTC-3′, *GAPDH-F* 5′-CAGCAACTCCCACTCTTCC-3′, *GAPDH-R* 5′-GGTCCAGGGTTTCTTACTCC-3′, *nestin-F* 5′-CTTTCAAGCCCTCGTGTC-3′, *nestin-R* 5′-ACACTATGAGGACGGAGGA-3′, *Sox-2-F* 5′-AGAGCAAGTACTGGCAAGACCGTT-3′, and *Sox-2-R* 5′-TACATGGATTCTCGGCAGCCTGAT-3′.

Quantitative Real-Time RT-PCR Analysis

Total RNA was extracted from the brain tissues which were collected from E12-P7 time points. Samples were grounded in liquid nitrogen. Next, RNA was extracted using an RNA simple total RNA extraction kit (TIANGEN, Beijing, DP419). First-strand cDNA was synthesized using reverse transcription kit (TIANGEN, Beijing, KR104). Real-time reverse transcription-polymerase chain reaction (RT-PCR) was carried out using the ViiA™ 7 Real-Time PCR System (Applied Biosystems) with SYBR® Select Master Mix (Applied Biosystems, 4472908). The primers of *pcdh11x* used were as described above. Transcript levels were normalized to the expression levels of *β-actin*, as determined using the primers as described above. Samples were run in three replicates for each gene expression assay. The sizes of the amplified fragments were confirmed by agarose gel electrophoresis.

RNA Interference Analysis

NSC spheres were collected and digested with Accutase® solution (Sigma-Aldrich, Saint Louis, MO, A6964) into single cells. Cells were prepared according to the protocol provided by Lonza, the manufacturer of the electrotransfection apparatus. We electrotransfected the *pcdh11x*-small interfering RNA (*siRNA*) and *nc-siRNA* into NSCs at 40 nM as previously described (Persengiev et al. 2004; Semizarov et al. 2003). We custom-ordered the following three siRNAs targeting the conserved sequence of mouse pcdh11x from GenePharma Co.: *pcdh11x*-mus-1346, sense 5′-GUCCCAUCAAUUGACAUAATT-3′ and anti-sense 5′-UUAUGUCAAUUGAUGGGACTT-3′; *pcdh11x*-mus-698, sense GCACCGUUAUUCCCAACAATT and anti-sense 5′-UUGUUGGGAAUAACGGUGCTT-3′; *pcdh11x*-mus-1707, sense 5′-GCCUUUCUGUUCCUGAGAATT-3′ and anti-sense 5′-UUCUCAGGAACAGAAAGGCTT-3′; negative control siRNA, sense 5′-UUCUCCGAACGUGUCACGUTT-3′ and anti-sense 5′-ACGUGACACGUUCGGAGAATT-3′. The anti-Pcdh11x siRNAs targeted sequences at positions 1346 to 1364 (no.

1346), 698 to 716 (no. 698), or 1707 to 1725 (no. 1707) on the Pcdh11x transcript.

DNA Constructions

The small hairpin RNA (shRNA) vectors targeting mouse Pcdh11x were synthesized from Neuron Biotech Co. The specific sequence targeting Pcdh11x was screened from the above experiment (*pcdh11x*-mus-698) and was cloned into lentivirus expression vector *PLKD-UbiC-GFP-U6-shRNA* (LiDR007A, Neuron Biotech Co.). Control nonsilencing shRNA is a negative control that is expressed under the control of the U6 promoter and contains no homology to known mammalian genes. The sequence of the negative control shRNA are F 5′-UUCUCCGAACGUGUCACGUTT-3′ and R 5′-ACGUGACACGUUCGGAGAATT-3′.

For construction of overexpression vector pCAG-pcdh11x-GFP, the target cDNA (BC126930) was obtained from Sango Biotech gene synthesis service and was cloned into pCAG-GFP (Addgene, 11150) with multiple cloning sites.

In utero Electroporation

In utero electroporation was performed with an electroporator (ECM830, BTX), delivering five 50-ms pulses of 50 V with 1-s intervals (Saito 2006; Woodhead et al. 2006). Pregnant CD1 mice were anesthetized with isoflurane, and their body temperature was monitored and maintained using a heating pad. We injected GFP expression plasmids driven by the U6 promoter, including the *PLKD-UbiC-GFP-U6-shRNA/shRNA*-negative control, *pcdh11x shRNA*, and plasmids driven by CAG promoter, including pCAG-GFP (negative control) and pCAG-pcdh11x-GFP. Approximately 1 μl of DNA solution (3 μg/μl) per embryo was mixed with Fast Green FCF (Sigma-Aldrich, Saint Louis, MO, F7258, 0.1 %) and was injected into the lateral ventricle at the indicated ages using a pulled glass micropipette.

Western Blot Analysis

E13.5 cortical progenitor cells were obtained as described above. Cells cultured in 100-mm dishes were transfected with *nc-shRNA*, *pcdh11x-shRNA*, and *pCAG-pcdh11x-GFP* vector, respectively, in the dose of 10–18 μg/dish. The samples were collected and washed in 0.01 M PBS; then, the cell pellet was lysed in lysis buffer (ProteoJET™ Mammalian Cell, Lysis Reagent, Fermentas, K0301) containing protease inhibitor cocktail (Halt™ protease inhibitor cocktail, EDTA-Free Thermo, 87785, 1:100). Cells were centrifuged at 20,000*g* for 15 min at 4 °C. Supernatants were collected and combined with 5× SDS sample buffer and boiled for 2–5 min. The resulting protein samples were applied to 8 % SDS-PAGE and transferred to PVDF membranes. The blots were blocked with 5 % milk in Tris-buffered saline with Tween 20 (TBS-T) buffer for 30 min and probed with the following primary antibodies: goat anti-Pcdh11x (Pcdh11x (E-13), Santa Cruz, sc-103726, 1:100 dilution in blocking regent), rabbit anti-β-actin (β-Actin (13E5) rabbit mAb, cell signaling, 4970, 1:1,000; dilution in blocking regent). Blots were washed three times with TBS-T buffer before incubation with HRP-conjugated donkey anti-goat antibody (peroxidase-conjugated AffiniPure Donkey Anti-Goat^{++} IgG (H+L), Jackson ImmunoResearch, 705-035-003, 1: 10,000) and HRP-conjugated goat anti-rabbit antibody (anti-rabbit IgG, HRP-linked antibody, cell signaling, 7074, 1:1,000). The signal was visualized using the ECL Western blotting system (BIO-RAD GelDoc 2000). To ensure equal loading, protein concentrations were determined using the BCA protein assay (Pierce™ BCA Protein Assay Kit, 23227). Densitometry of scanned films was performed with ImageJ.

Fluorescence-activated cell sorting (FACS) Analysis

After transfection with *nc-shRNA*, *pcdh11x-shRNA*, *pCAG-GFP*, and *pCAG-pcdh11x-GFP* vectors into NSCs, cells were collected and prepared into single-cell suspensions, then were analyzed for apoptosis assays with Moflo XDP flow cytometry (Beckman Coulter, Inc.) equipped with analyzing software (Summit 5.3, Beckman Coulter, Inc.). The apoptosis assay was achieved using annexin V-PE/7-AAD apoptosis detection kit (Annexin V-PE Apoptosis Detection Kit I, BD, Franklin Lakes, NJ, 559763). We prepared samples as per the manufacturers' operating instructions. Each gating that divided antigen-positive or antigen-negative fractions was made by comparing stained areas with negative control isotype IgGs. The percentage of cells positive for each antigen was evaluated by at least three independent experiments.

Morphometric Analysis and Cell Population Quantification

Stereological analysis of the number of cells was performed using confocal microscopy (Leica SP5 II) to analyze all series of coronal sections, to count cells expressing the indicated marker throughout the SVZ and cortical plate (CP) regions. The total estimated number of cells within the SVZ and CP regions that were positive for each of the indicated markers was obtained multiplying the average number of positive cells per section (approximately 20–30 sections) (Farioli-Vecchioli et al. 2008; Gould et al. 1999; Jessberger et al. 2005). The Image-Pro Plus software was used to count labeled cells.

Statistical Analysis

Statistical analysis was performed using SPSS 13.0 software (SPSS Inc.). Data were analyzed by independent sample *t* test or one-way ANOVA. Unless otherwise indicated,

experimental results were expressed as mean ± standard error (SEM). $P<0.05$ was considered statistically significant. We used Prism software to generate the graphics.

Results

Expression Pattern of Pcdh11x in the Adult and Embryonic Mouse Brain

During cortical development, neural stem cells produce neurons and glial cells through asymmetric division (Leber et al. 1990). First, to address where Pcdh11x is expressed in the brain, we used immunochemistry to determine the localization of Pcdh11x. We found that Pcdh11x was predominantly expressed in the subcortex and hypothalamus (Fig. 1a, b). The antibody blocking peptide was available for testing the specificity of the Pcdh11x antibody (Fig. 1a–c, right panel).

To test the transcriptional expression of Pcdh11x in the brain, we detected localization of Pcdh11x during embryonic and adult phase through immunofluorescence and PCR methods. Tissue samples from the adult VZ/SVZ, hippocampus, cortex, heart, liver, and kidney were used to assay the levels of Pcdh11x transcripts. Pcdh11x mRNA was predominantly expressed in the brain rather than in the peripheral tissues (Fig. 2a). The results were similar to some previous studies which suggested that little Pcdh11x transcription could be detected from some peripheral tissues (heart, liver, and kidney) (Blanco et al. 2000; Ahn et al. 2010). In the following steps, we examined the distribution of Pcdh11x in different regions of the adult mouse brain. The results showed that there were only minor differences in the transcriptional level of Pcdh11x among several regions (Fig. 2b).

To determine whether Pcdh11x is located in neurons or astrocytes, we double stained adult slices with anti-neuN or anti-GFAP and anti-Pcdh11x. As shown in Fig. 2c, Pcdh11x and GFAP were expressed at the different brain regions. In Fig. 2d, we found that in the subcortex, Pcdh11x colocalized with some of $NeuN^+$ interneurons. The results prompted us to consider the possible function of Pcdh11x on neurons. To

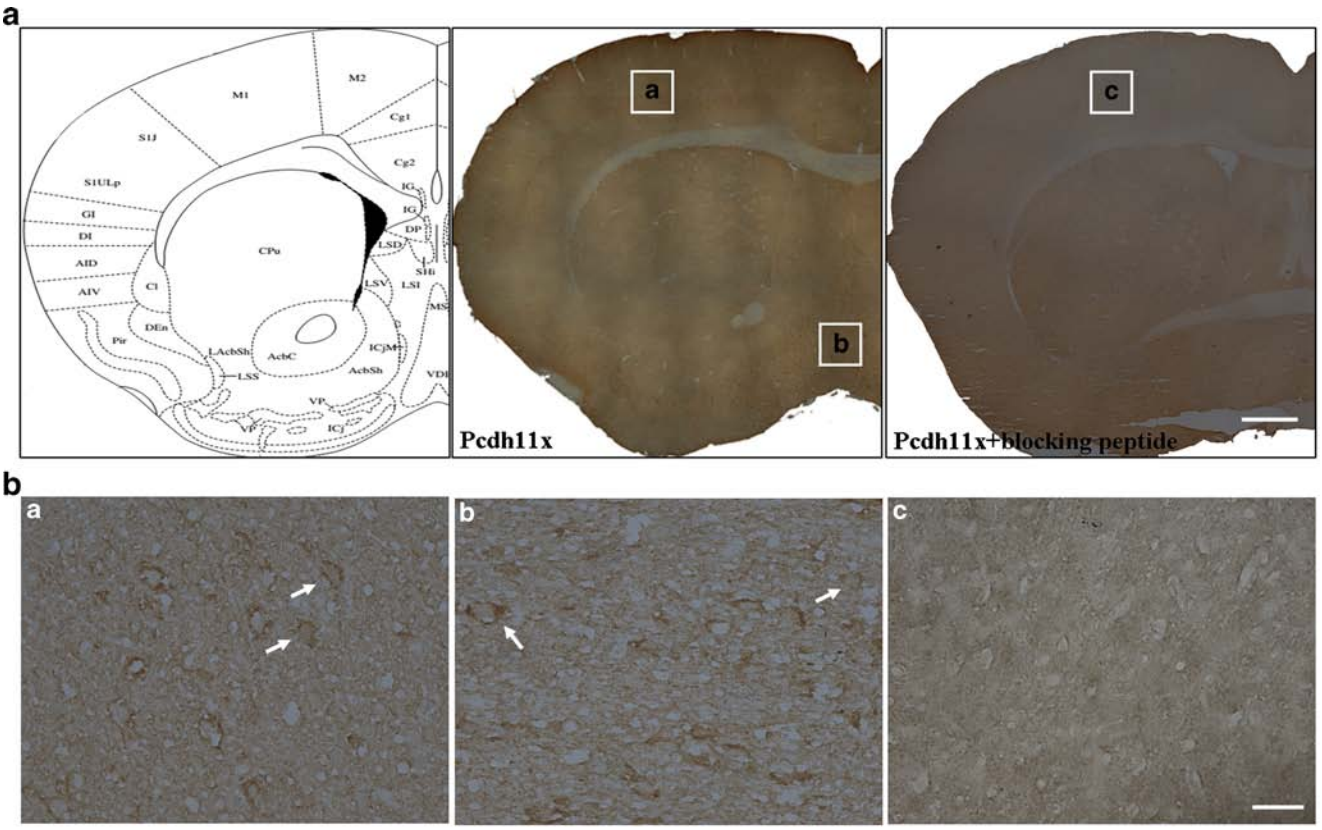

Fig. 1 Pcdh11x is expressed at the different brain regions in adult mice (**a**). *Left panel* schematic of brain regions for immunochemical analysis. *S1ULP* primary somatosensory cortex, upper lip region; *S1J* primary somatosensory cortex, jaw region; *M1* primary motor cortex; *Pir* piriform cortex; *Ms* medial septal nucleus; *VDB* nucleus of the vertical limb of the diagonal band; *Mfb* medial forebrain bundle; *VP* ventral pallidum. *Middle panel* representative images of immunostaining Pcdh11x in adult mice. Pcdh11x is mainly expressed in subcortex and hypothalamus. *Right panel* representative images of anti-Pcdh11x with blocking peptide which was available for competition studies. *Scale bars* 100 μm (**b**). Higher magnifications are shown by *white boxes* (*a*). The *white boxes a* and *b* indicate the subcortex area and hypothalamus area where Pcdh11x was positively expressed, respectively. The *white arrows* show the Pcdh11x-positive cells. *Scale bars* 20 μm. The *white box c* indicates the subcortex area from anti-Pcdh11x and blocking peptide treated group where Pcdh11x was negatively expressed. *Scale bars* 20 μm

further test the specificity of Pcdh11x antibody, we transfected HEK 293T cells with *pCAG-pcdh11x-GFP* and the negative control vectors. After 48 h, we stained the cells with anti-Pcdh11x. We found that signals of *pCAG-pcdh11x-GFP* overlapped with the anti-Pcdh11x. Cells accepting *pCAG-GFP* (negative control) vectors negatively stained with anti-Pcdh11x (Fig. 2e). These results indicated that Pcdh11x was primarily expressed in the central nervous system and predominantly expressed in neurons rather than astrocytes.

Expression Curves of Pcdh11x and Correlation between Pcdh11x and Neural Stem Cells

To determine the developmental expression pattern of Pcdh11x, the levels of Pcdh11x expression in the brain tissues (cortex, hippocampus, and VZ/SVZ regions), normalized to β-actin, were measured at different time points (E12, E14, E16, E18, P1, P4, and P7) by real-time PCR (Fig. 3). In the cortex, Pcdh11x expression was detected dispersed at each time point, and it was strongly expressed at P4 and expressed

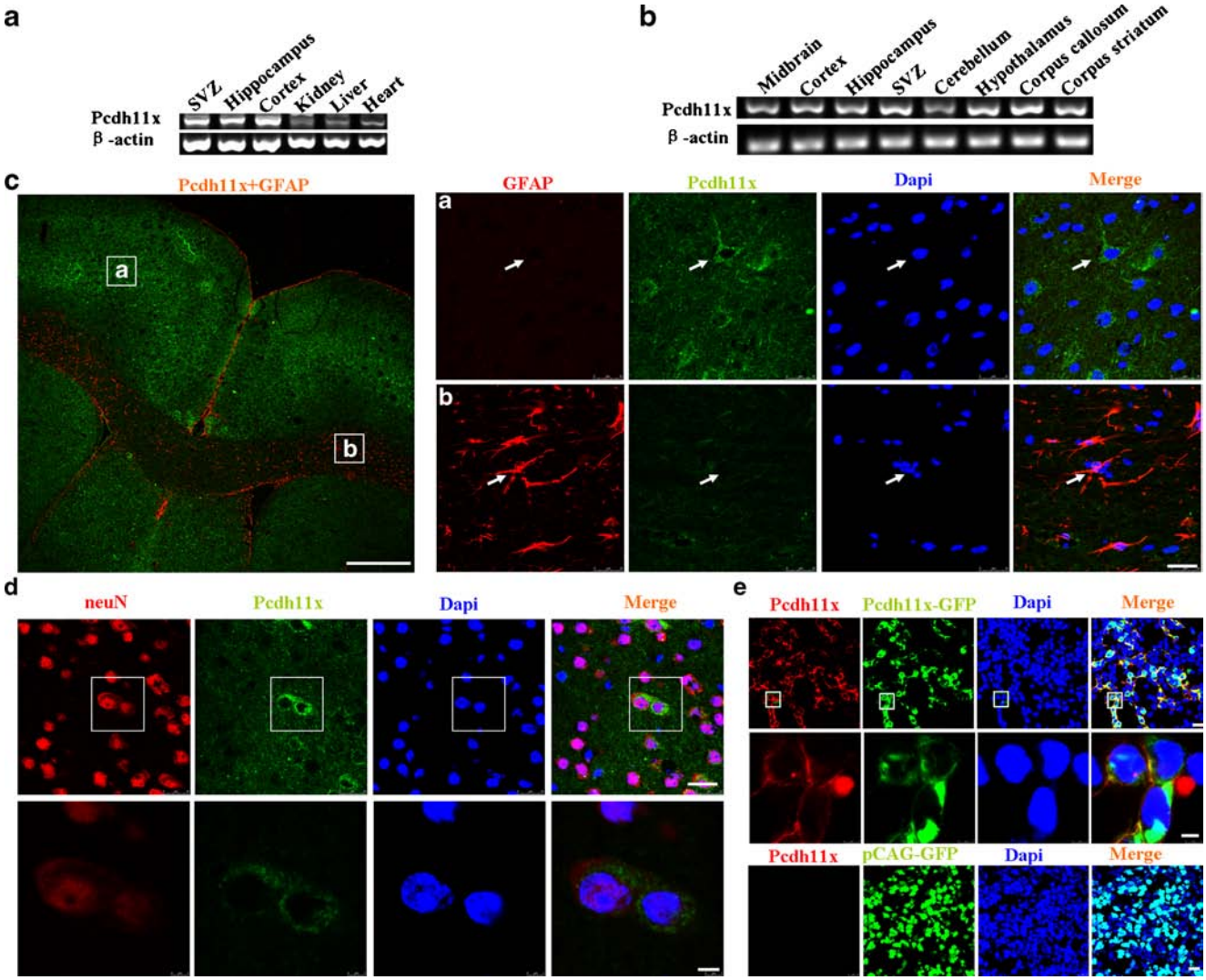

Fig. 2 Pcdh11x is expressed in NeuN$^+$ neurons but not in GFAP$^+$ cells (**a**). Pcdh11x is predominantly expressed in mouse brain. RT-PCR expression analysis of Pcdh11x levels at different mouse tissues including the SVZ, hippocampus, cortex, kidney, liver, and heart. β-actin as internal uploading control (**b**). RT-PCR expression analysis of Pcdh11x levels at different brain regions: midbrain, cortex, hippocampus, SVZ, cerebellum, hypothalamus, corpus callosum, and corpus striatum (**c**, **d**). Pcdh11x is located in the neuron but not in GFAP-immunoreactive cells. Representative immunofluorescence images of adult mouse subcortex and corpus callosum (**c**). *Scale bars* 500 μm. The *boxes a* and *b* indicate high-magnification images (**d**) of the boxed areas in *panel c*. The *white arrows* in *a* indicate that cells express Pcdh11x$^+$ alone; the *white arrows* in *b* indicate that cells express GFAP$^+$ alone. *Scale bars* 25 μm. The images show that Pcdh11x (*green*) is expressed in some of NeuN-positive interneurons (*red*) (*box* indicated). *Scale bars* 25 μm; the *bottom panel* shows higher magnification of the boxed areas in *upper panel* in **d**. *Scale bars* 5 μm. **e** Immunofluorescence analysis of specifity of anti-Pcdh11x at HEK 293T cells with *pCAG-pcdh11x-GFP*. Images in the *upper row* display *pCAG-pcdh11x-GFP* (*green*) and Pcdh11x (*red*). *Scale bars* 25 μm. *Middle panel* images show the higher magnification of the boxed regions of the *upper panel* images. *Bottom panel* images show that *pCAG-GFP* did not colocalize with Pcdh11x (*red*). Boxed area *scale bars* 5 μm

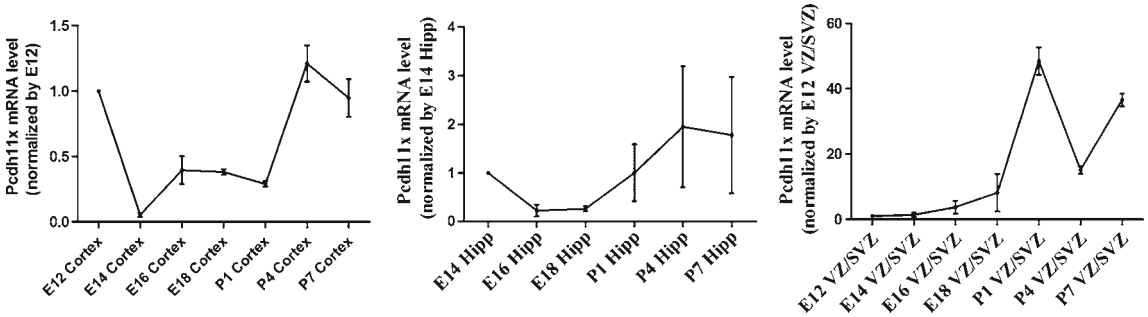

Fig. 3 Quantification of Pcdh11x in the cortex, hippocampus, and VZ/SVZ regions (**a**, **b**, **c**). Real-time PCR was used to analyze the expression of Pcdh11x in the cortex, hippocampus, and VZ/SVZ regions, using the $2^{-\Delta\Delta Ct}$ method. The gene expression was normalized to those β-actins. *Error bars* represent the SD of three independent experiments, which were each performed in three duplicates. *HIPP* hippocampus

at lower levels at E14 (Fig. 3a). In the hippocampus, Pcdh11x weakly expressed at embryonic stages; however, in the postnatal hippocampus, Pcdh11x gradually increased in strong expression at P4 and P7 (Fig. 3b). In the VZ/SVZ region, Pcdh11x expression gradually increased from E14 to P1 and then decreased (Fig. 3c). It is worth noting that the mean expression levels of Pcdh11x reflect heterogeneity among the cortex, hippocampus, and VZ/SVZ regions.

The expression pattern of *pcdh11x* at different time points indicated that Pcdh11x may have important functions in the central nervous system. To address whether Pcdh11x is expressed on neural stem cells we double stained anti-Pcdh11x and anti-nestin in cultured NSCs and E16 mouse brain tissues. We found that Pcdh11x was colocalized with nestin (Fig. 4a). In addition, we double stained anti-Pcdh11x and anti-Sox-2 in NSCs and E14 tissue slices and found that Pcdh11x and Sox-2 were colocalized (Fig. 4a–b).

Next, we examined the levels of Pcdh11x and stem cell markers, nestin, and Sox-2, in NSCs by RT-PCR. The results showed that NSC positively expressed Pcdh11x with nestin and Sox-2 (Fig. 4b). These results suggested that Pcdh11x may affect the neural development process.

Pcdh11x Decreases Neural Differentiation and Premature Migration but Increases Neural Proliferation

To further test the function of Pcdh11x in the nervous system, transient transfection with siRNA/shRNA targeting Pcdh11x was used. We performed the real-time PCR and Western blot

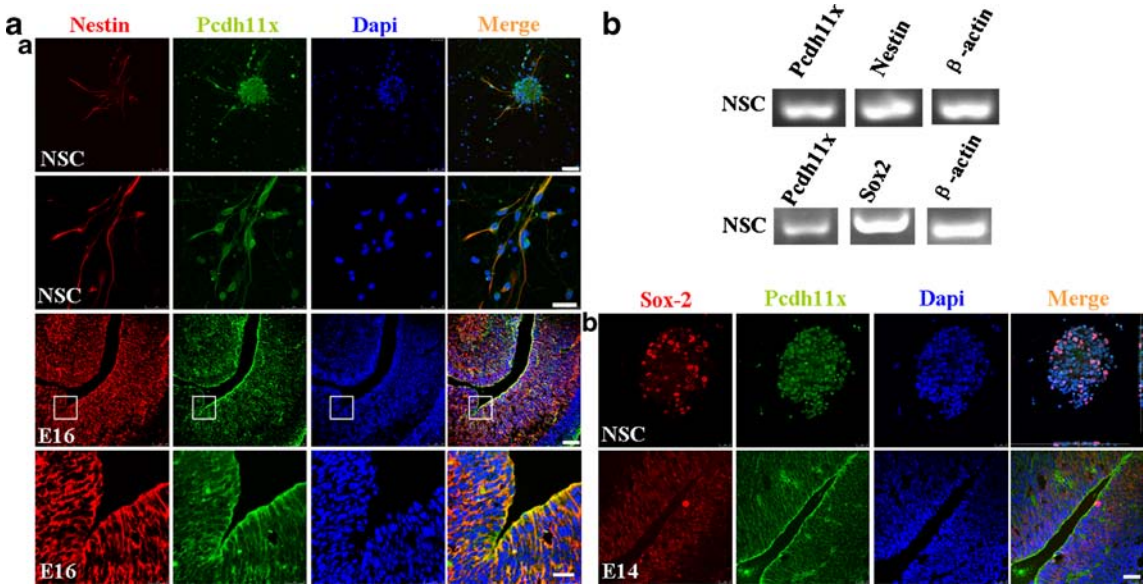

Fig. 4 Pcdh11x is expressed in neural stem cells (**a**). Representative confocal image of Pcdh11x in neural stem cells and tissues *a*. The *upper row* images show neural stem cell spheres at low magnification. *Scale bars* 50 μm. The *second row* images show neural stem cells at high magnification. *Scale bars* 25 μm. The *third row* images show the E16 VZ/SVZ region of the mouse brain. *Scale bars* 100 μm. The *fourth row* images show the E16 VZ/SVZ region of the mouse brain at higher magnification. *Scale bars* 25 μm. *b* The *upper row* images show neural stem cell spheres at higher magnification. *Scale bar* 100 μm. The *second row* shows the E14 VZ/SVZ region of the mouse brain. *Scale bar* 100 μm. **b** Transcripts expression of *pcdh11x* and *nestin*; *Sox-2* in neural stem cells

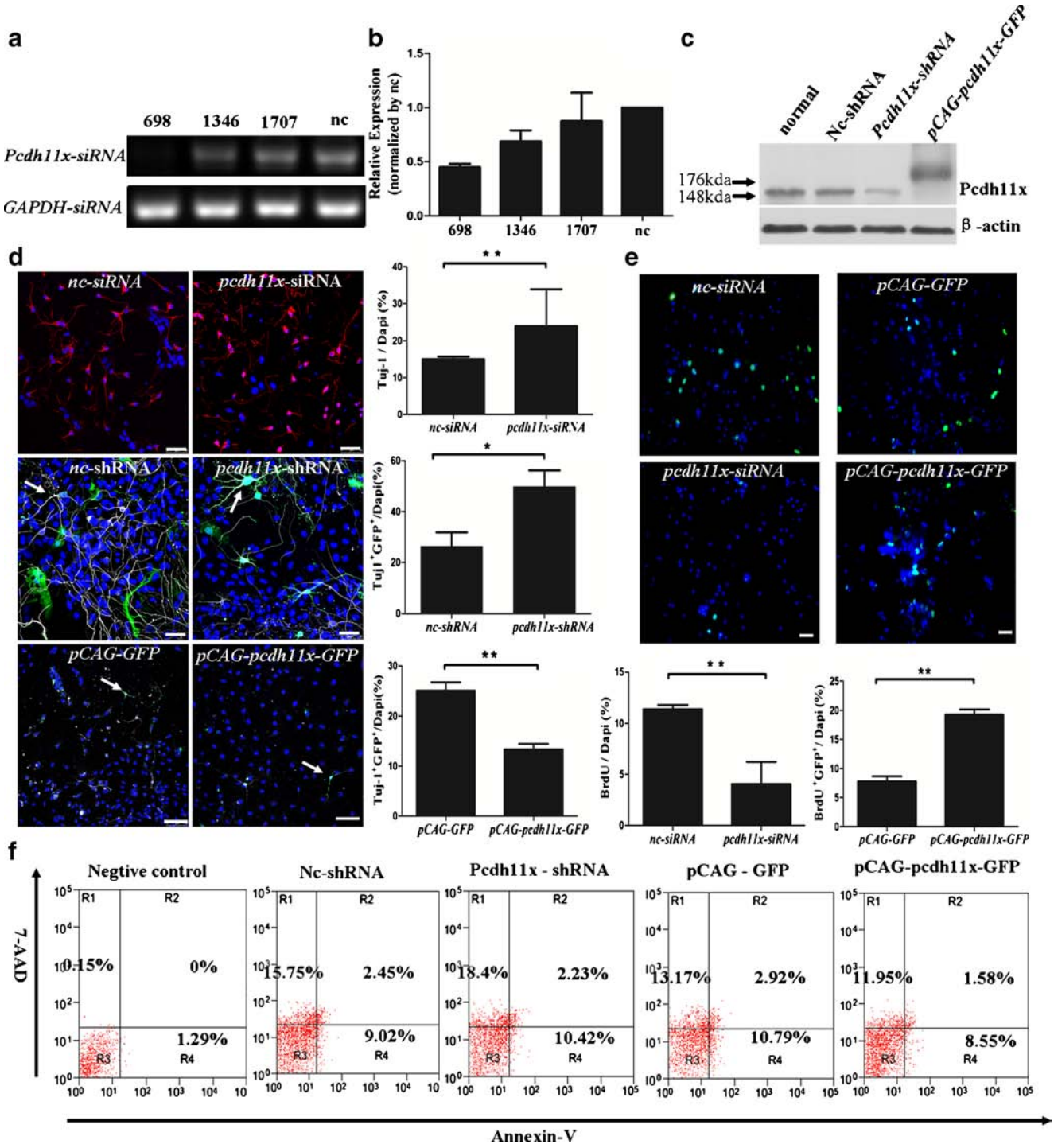

experiment. We first customized three *pcdh11x siRNA* constructs including 698, 1,346, and 1,707 isoforms in RNA interference experiment. The results showed that the 698 siRNA construct is specific in reducing the expression of *pcdh11x* gene (Fig. 5a, b). The Pcdh11x siRNA/shRNA caused about a half reduction in the expression of Pcdh11x in neural stem cells (Fig. 5b). Furthermore, we transfected neural stem cells with *pCAG-pcdh11x-GFP* to increase the protein level of Pcdh11x. We found that overexpression of Pcdh11x, as a fusion protein, caused an increase in the expression of Pcdh11x in neural stem cells (Fig. 5c).

To examine whether Pcdh11x regulates embryonic neural stem cell proliferation and differentiation, primary embryonic neural stem cells were freshly derived from E13.5 mouse brains and transfected with *Pcdh11x shRNA/siRNA* and *pCAG-pcdh11x-GFP* to increase the protein level or inhibit the activity of Pcdh11x, respectively. After 5 days, we found that *pcdh11x-siRNA/shRNA* group promoted neuronal

◀ **Fig. 5** Pcdh11x is essential for neural differentiation and proliferation (**a**–**c**). siRNAs/shRNAs-Pcdh11x suppress Pcdh11x expression. **a** RNAs extracted from neural stem cells transfected with *nc-siRNA* (control) were compared with RNAs from neural stem cells transfected with Pcdh11x-siRNAs (698, 1,346, and 1,707) by real-time PCR using primers specific for Pcdh11x (*top*) or GAPDH (*bottom*). **b** Quantification of relative expression in **a**. *Error bar* means the SD of three independent experiments, which were each performed in three duplicates. **c** Western blot analysis for expression of Pcdh11x (*top*) of protein extracts from neural stem cells cultures transfected with *nc-shRNA* (control), *Pcdh11x-shRNA* (with the same sequence as 698-siRNA) and *pCAG-pcdh11x-GFP*. **d** *Left panel* representative images of Tuj-1-positive (Tuj-1$^+$) cells in control, *pcdh11x-siRNA* (*pcdh11x-shRNA*) and *pCAG-pcdh11x-GFP* treated neural stem cells. Tuj-1, *red* (shRNA group, overexpression group, *white*); Dapi, *blue*. The *white arrowheads* indicate GFP$^+$ and Tuj-1$^+$ cells. *Scale bars* 50 μm; *pCAG-GFP*, *pCAG-Pcdh11x-GFP*, *Scale bars* 100 μm. *Right panel* quantification of the Tuj-1 (Tuj-1$^+$)-positive cells in control, *pcdh11x-siRNA* (*pcdh11x-shRNA*) and *pCAG-pcdh11x-GFP* treated neural stem cells. *Error bars* indicate the SEM of the mean. $^{**}P<0.01$ and $^{*}P<0.05$ by an independent sample *t* test. Around 2,000 cells were quantified. **e** BrdU-positive (BrdU$^+$) cells in control, *pcdh11x-siRNA* (*pcdh11x-shRNA*) and *pCAG-pcdh11x-GFP* treated neural stem cells. *Upper panels* representative images, *Scale bars* 30 μm. *Lower panel* quantification of BrdU$^+$ cells in control, *pcdh11x-siRNA* (*pcdh11x-shRNA*) and *pCAG-pcdh11x-GFP* treated neural stem cells. *Error bars* indicate the SEM. $^{**}P<0.01$ by an independent sample *t* test. Around 1,500 cells were quantified. **f** Flow cytometric analysis of apoptosis cells using annexin V-PE/7-AAD apoptosis detection kit. Annexin V positive, meanwhile, 7-AAD negative shows early apoptotic death cells

differentiation dramatically, leading to a considerable increase in the percent of Tuj1-positive neurons at day 5 of differentiation ($P<0.01$) (Fig. 5d). Transfection of *pCAG-pcdh11x-GFP* also decreased neuronal differentiation ($P<0.05$) (Fig. 5d). These results indicated that Pcdh11x inhibited neuronal differentiation of neural stem cells. Cell proliferation was determined by BrdU labeling of dividing cells. Transfection of Pcdh11x led to a dramatic increase of cell proliferation ($P<0.01$) (Fig. 5e).

To eliminate the possibility that apoptosis may be affecting the above results, we did FACS experiment to examine the expression of annexin V in the treated NSCs (Fig. 5f). We detected that the rate of early apoptotic death cells in shRNA groups and overexpression groups has no significant difference between the two groups.

The embryonic SVZ is a critical site for generating cortical excitatory neurons (Noctor et al. 2004; Haubensak et al. 2004), which are in turn generated in the VZ by asymmetric division (Kowalczyk et al. 2009; Noctor et al. 2001). Pax6, Tbr2, Tbr1, and Ctip2 are expressed sequentially in the neurogenesis of glutamatergic neurons. To obtain further in vivo evidence for the function of Pcdh11x, we examined the migration and differentiation of cells following in utero electroporation of shRNA or overexpression vectors against Pcdh11x. The number of radial glia/apical progenitors (Pax6$^+$) increased, whereas the production of Ctip2$^+$ layer V and VI neurons, Tbr1$^+$ layer VI neurons, and Tbr2$^+$ basal progenitors was significantly reduced in the cortex compared with the control (Fig. 6a–d), implying that Pcdh11x impaired early neurogenesis and severely affected the generation of deep layer neurons. Pcdh11x also decreased cell migration from the VZ/SVZ regions (Fig. 6e–f). To sum up, Pcdh11x decreased premature cell migration to the cortical plate. During neural development, neural stem cells rest in the VZ/SVZ and migrate out into cortical plate upon differentiation. To determine whether Pcdh11x influences neural stem cell proliferation and differentiation in the embryonic brains, we inhibited or increased the expression of Pcdh11x in neural stem cells in the VZ of E13.5 mouse brains by in utero electroporation. The electroporated brains were analyzed at E17.5. Cells that had taken up Pcdh11x shRNA or overexpression vectors were labeled green by coexpression of green fluorescent protein (GFP). Pcdh11x led to a marked increase of cells that were positively labeled for Ki-67, a proliferative marker, as revealed by increased Ki-67$^+$ GFP$^+$ cells (Fig. 6g, h). These results suggest that Pcdh11x promote neural stem cell proliferation.

Discussion

Our experiments indicate that Pcdh11x is primarily expressed in the central nervous system and plays an important role in brain development (Figs. 2a, b, 3, 5, and 6). The results were similar to the previous results which Pcdh11x varies from one region of the brain to another (Blanco et al. 2000). Previous studies have used the RT-PCR (Blanco et al. 2000; Blanco-Arias et al. 2004) or northern blotting (Yoshida and Sugano 1999) methods to detect the expression of Pcdh11x in humans. Pchd11x is widely distributed in some neuronal areas (Priddle and Crow 2013), which is consistent with our results. In addition, we found that Pcdh11x is primarily expressed in neurons rather than astrocytes (Fig. 2c, d). Previous studies using tyrosine hydroxylase (TH) immunostaining have shown that Pchd11x-positive neurons are TH negative (Hertel et al. 2008). Our results suggested that the expression pattern of Pcdh11x and its expression curve at different time points indicate that Pcdh11x is primarily expressed in the brain at similar levels across the cortex, hippocampus, and VZ/SVZ regions, which agrees with a previous report (Blanco et al. 2000). And, our immunostaining results indicate abundant Pcdh11x-positive areas in the cortex and hypothalamus (Fig. 1). These results were corroborated by the existing literature (Blanco et al. 2000; Hertel et al. 2008; Priddle and Crow 2013). This paper mapped the expression in embryonic and adult mouse brains. Although commercial polyclonal antibody to Pcdh11x exists, there have been no immunohistochemical or immunofluorescence studies to address Pcdh11x expression in the mouse brain. However, one study published in 2013 did examine expression in the human brain

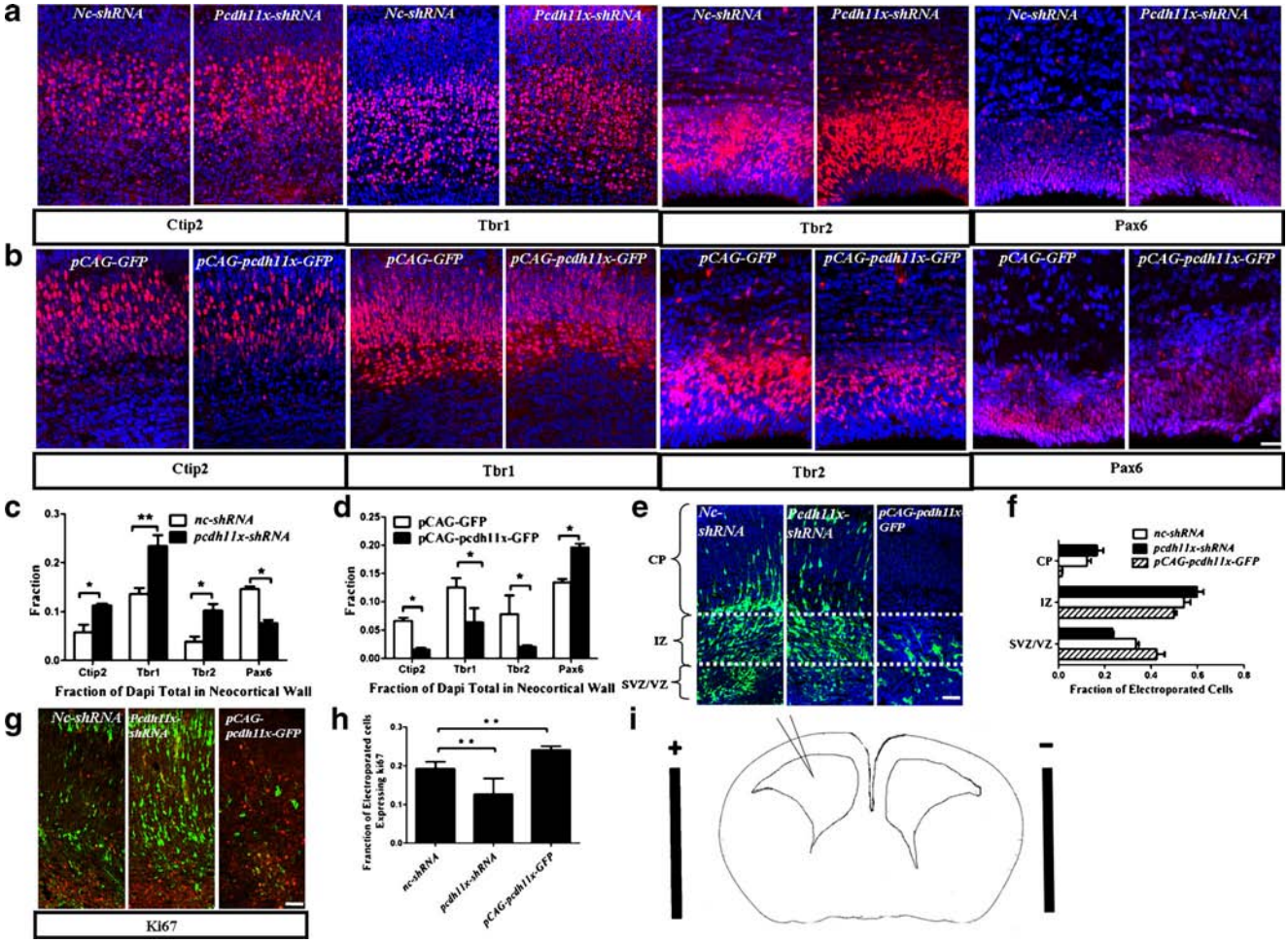

Fig. 6 Pcdh11x decreased neural differentiation and premature migration, but increased neural proliferation (**a**, **b**). Representative confocal images of Ctip2, Tbr1, Tbr2, and Pax-6 at E14 mouse forebrain that was coelectroporated in utero with the nonsilencing shRNA construct (control) and *pcdh11x-shRNA* or *pCAG-GFP* (control) and cDNA vector (*pCAG-pcdh11x-GFP*). Electroporated cells are *green*, and Ctip2, Tbr1, Tbr2, and Pax6 stained *red*. *Scale bars* 100 μm. **c**, **d** Quantification of the positive fraction of Dapi total in neocortical wall in **a** and **b**, respectively. *Error bars* indicate the SEM. **P*<0.05 and ***P*<0.01 by an independent sample *t* test. control *n*=4 brains, 1,630 cells; shRNA *n*=3 brains, 1,439 cells; *pCAG-GFP n*=4 brains, 1,800 cells; *pCAG-pcdh11x-GFP n*=4 brains, 1,890 cells (**e**). Pcdh11x decreased premature migration from the VZ region. Electroporated cells are green and Dapi staining blue in representative confocal images. *Scale bars*, 100 μm. *CP* cortical plate, *IZ* intermediate zone, *VZ/SVZ* ventricular/subventricular zone. **f** Quantification of fraction of total electroporated cells found in each brain region in e. Control *n*=4 brains, 1,660 cells; shRNA *n*=4 brains, 1,750 cells; *pCAG-pcdh11x-GFP n*=4 brains, 1,200 cells (**g**). Pcdh11x increased neural proliferation. Embryos at E14 were electroporated nonsilencing shRNA construct (control) and shRNA targeting pcdh11x (*pcdh11x-shRNA*) or pCAG-GFP (control) and cDNA vector (*pCAG-pcdh11x-GFP*). Electroporated cells (*green*) and Ki-67 (*red*). *Scale bars* 100 μm (**h**). Quantification of the proportion of electroporated cells expressing Ki-67. ** indicates *P*<0.01 by one-way ANOVA. *n*=4 brains each, 4,600 cells total (**i**). Schematic of electroporation protocol: DNA vectors are injected into the ventricle and are introduced into the adjacent neuroepithelial cells, which are directed toward the positive electrode. The positive electrode is aligned outside the brain as shown

(Priddle and Crow 2013). We confirmed the specificity of the antibody before carrying out all the experiments by transfecting the pCAG-pcdh11x-GFP vectors to 293T cell line (Fig. 2e) and using the antibody blocking peptide (Fig. 1).

A longitudinal study of Pcdh11x in the prefrontal cortex has shown that levels of Pcdh11x are highest in male neonates, decrease through childhood, and are lowest in adults of both sexes (Weickert et al. 2009). In the mouse brain, we identified the expression in the cerebral cortex, hippocampus, and VZ/SVZ regions using RT-PCR. In the cortex, we detected the mRNA expression of Pcdh11x at some time points from E12 to P7. In our experiments, Pcdh11x mRNA was strongly expressed at E12 and decreased from E14 to P1. At P4, the Pcdh11x mRNA was again strongly expressed, as was the case for postnatal stage P7. In the hippocampus, the mRNA of Pcdh11x was highly expressed at P4 and P7, weakly expressed from E14 to E18, and then increased from P1. In the VZ/SVZ, Pcdh11x mRNA expression gradually increased from E14 to P1 and then fluctuated at P4 and P7 (Fig. 3).

Our interference experiment studied the function of Pcdh11x on neural stem cells. The results of WB and real-time PCR manifest that 698-siRNA is activated and specific.

This study demonstrates that Pcdh11x has an important role in embryonic neural stem cell proliferation and differentiation during neural development. Overexpression of Pcdh11x in embryonic neural stem cells leads to reduced neural stem cell differentiation, as well as enhanced neural proliferation. We provide strong evidence that Pcdh11x is an essential regulator of neurogenesis during multiple developmental stages and the important role of Pcdh11x in embryonic brains is established in this study. Proper microenvironments or niches regulate the specification, self-renewal, and differentiation of stem cells (Fuchs et al. 2004; Zhang et al. 2010). In the developing cerebral cortex, the neural stem cells could provide their own supportive environment in development (Zhang et al. 2010). In this paper, we observed that reduction of Pcdh11x resulted in increased cell migration from the VZ and premature neuronal differentiation (Fig. 6). This result supports that Pcdh11x mediates the attachment of stem cells to their niches. Cortical development normally depends on the sequential production of each laminar cell type (Rash et al. 2011; Walsh and Reid 1995). Reduction of Pcdh11x that decreased Pax-6-positive cells and increased other laminar cell type numbers showed that more precursor cells migrated to cortical plate. In addition, overexpression of Pcdh11x produced inverse results. In conclusion, our study demonstrated that Pcdh11x regulates neural differentiation and proliferation both in vitro and in vivo and provides new insights into the function of Pcdh11x in neural differentiation, premature migration, and neural proliferation. However, detailed molecular mechanisms merit further investigation.

Acknowledgments This study was funded by Military Medical Project (BWS11J002, BWS12J010) and National Natural Science Foundation (no. 30973096). Thanks to Zhang Xiao Chong at Ju Lu Hospital for her help with the experiment. We thank Elsevier Language Editing (Project no.: 39443) for assisting in the preparation of this manuscript. The authors would like to thank all the anonymous reviewers for their valuable comments on how to improve the quality of this paper.

Conflict of Interest No conflicts of interest, financial or otherwise, are declared by the authors.

References

Ahn K, Huh JW, Kim DS, Ha HS, Kim YJ, Lee JR, Kim HS (2010) Quantitative analysis of alternative transcripts of human PCDH11X/Y genes. Am J Med Genet B Neuropsychiatr Genet 153B:736–744

Barnabe-Heider F, Wasylnka JA, Fernandes KJ, Porsche C, Sendtner M, Kaplan DR, Miller FD (2005) Evidence that embryonic neurons regulate the onset of cortical gliogenesis via cardiotrophin-1. Neuron 48:253–265

Benson DL, Colman DR, Huntley GW (2001) Molecules, maps and synapse specificity. Nat Rev Neurosci 2:899–909

Blanco P, Sargent CA, Boucher CA, Mitchell M, Affara NA (2000) Conservation of PCDHX in mammals; expression of human X/Y genes predominantly in brain. Mamm Genome 11:906–914

Blanco-Arias P, Sargent CA, Affara NA (2004) Protocadherin X (PCDHX) and Y (PCDHY) genes; multiple mRNA isoforms encoding variant signal peptides and cytoplasmic domains. Mamm Genome 15:41–52

Bozdagi O, Shan W, Tanaka H, Benson DL, Huntley GW (2000) Increasing numbers of synaptic puncta during late-phase LTP: N-cadherin is synthesized, recruited to synaptic sites, and required for potentiation. Neuron 28:245–259

Bruses JL (2000) Cadherin-mediated adhesion at the interneuronal synapse. Curr Opin Cell Biol 12:593–597

Farioli-Vecchioli S, Saraulli D, Costanzi M, Pacioni S, Cina I, Aceti M, Micheli L, Bacci A, Cestari V, Tirone F (2008) The timing of differentiation of adult hippocampal neurons is crucial for spatial memory. PLoS Biol 6:e246

Frank M, Kemler R (2002) Protocadherins. Curr Opin Cell Biol 14:557–562

Fuchs E, Tumbar T, Guasch G (2004) Socializing with the neighbors: stem cells and their niche. Cell 116:769–778

Gould E, Reeves AJ, Fallah M, Tanapat P, Gross CG, Fuchs E (1999) Hippocampal neurogenesis in adult Old World primates. Proc Natl Acad Sci U S A 96:5263–5267

Haubensak W, Attardo A, Denk W, Huttner WB (2004) Neurons arise in the basal neuroepithelium of the early mammalian telencephalon: a major site of neurogenesis. Proc Natl Acad Sci U S A 101:3196–3201

Hertel N, Krishna K, Nuernberger M, Redies C (2008) A cadherin-based code for the divisions of the mouse basal ganglia. J Comp Neurol 508:511–528

Hirabayashi Y, Itoh Y, Tabata H, Nakajima K, Akiyama T, Masuyama N, Gotoh Y (2004) The Wnt/beta-catenin pathway directs neuronal differentiation of cortical neural precursor cells. Development 131:2791–2801

Hirano S, Yan Q, Suzuki ST (1999) Expression of a novel protocadherin, OL-protocadherin, in a subset of functional systems of the developing mouse brain. J Neurosci 19:995–1005

Jessberger S, Romer B, Babu H, Kempermann G (2005) Seizures induce proliferation and dispersion of doublecortin-positive hippocampal progenitor cells. Exp Neurol 196:342–351

Kim SY, Yasuda S, Tanaka H, Yamagata K, Kim H (2011) Non-clustered protocadherin. Cell Adhes Migr 5:97–105

Kowalczyk T, Pontious A, Englund C, Daza RA, Bedogni F, Hodge R, Attardo A, Bell C, Huttner WB, Hevner RF (2009) Intermediate neuronal progenitors (basal progenitors) produce pyramidal-projection neurons for all layers of cerebral cortex. Cereb Cortex 19:2439–2450

Leber SM, Breedlove SM, Sanes JR (1990) Lineage, arrangement, and death of clonally related motoneurons in chick spinal cord. J Neurosci 10:2451–2462

Lopes AM, Ross N, Close J, Dagnall A, Amorim A, Crow TJ (2006) Inactivation status of PCDH11X: sexual dimorphisms in gene expression levels in brain. Hum Genet 119:267–275

Luckner R, Obst-Pernberg K, Hirano S, Suzuki ST, Redies C (2001) Granule cell raphes in the developing mouse cerebellum. Cell Tissue Res 303:159–172

Morishita H, Yagi T (2007) Protocadherin family: diversity, structure, and function. Curr Opin Cell Biol 19:584–592

Noctor SC, Flint AC, Weissman TA, Dammerman RS, Kriegstein AR (2001) Neurons derived from radial glial cells establish radial units in neocortex. Nature 409:714–720

Noctor SC, Martinez-Cerdeno V, Ivic L, Kriegstein AR (2004) Cortical neurons arise in symmetric and asymmetric division zones and migrate through specific phases. Nat Neurosci 7:136–144

Persengiev SP, Zhu X, Green MR (2004) Nonspecific, concentration-dependent stimulation and repression of mammalian gene expression by small interfering RNAs (siRNAs). RNA 10:12–18

Priddle TH, Crow TJ (2013) Protocadherin 11X/Y a human-specific gene pair: an immunohistochemical survey of fetal and adult brains. Cereb Cortex 23:1933–1941

Rash BG, Lim HD, Breunig JJ, Vaccarino FM (2011) FGF signaling expands embryonic cortical surface area by regulating Notch-dependent neurogenesis. J Neurosci 31:15604–15617

Redies C (2000) Cadherins in the central nervous system. Prog Neurobiol 61:611–648

Redies C, Vanhalst K, Roy F (2005) delta-Protocadherins: unique structures and functions. Cell Mol Life Sci 62:2840–2852

Saito T (2006) In vivo electroporation in the embryonic mouse central nervous system. Nat Protoc 1:1552–1558

Semizarov D, Frost L, Sarthy A, Kroeger P, Halbert DN, Fesik SW (2003) Specificity of short interfering RNA determined through gene expression signatures. Proc Natl Acad Sci U S A 100:6347–6352

Shapiro L, Colman DR (1999) The diversity of cadherins and implications for a synaptic adhesive code in the CNS. Neuron 23:427–430

Speevak MD, Farrell SA (2011) Non-syndromic language delay in a child with disruption in the Protocadherin11X/Y gene pair. Am J Med Genet B Neuropsychiatr Genet 156B:484–489

Suzuki ST (1996) Protocadherins and diversity of the cadherin superfamily. J Cell Sci 109(Pt 11):2609–2611

Tanaka H, Shan W, Phillips GR, Arndt K, Bozdagi O, Shapiro L, Huntley GW, Benson DL, Colman DR (2000) Molecular modification of N-cadherin in response to synaptic activity. Neuron 25:93–107

Vanhalst K, Kools P, Staes K, van Roy F, Redies C (2005) delta-Protocadherins: a gene family expressed differentially in the mouse brain. Cell Mol Life Sci 62:1247–1259

Walsh C, Reid C (1995) Cell lineage and patterns of migration in the developing cortex. CIBA Found Symp 193:21–40, discussion 59–70

Weickert CS, Elashoff M, Richards AB, Sinclair D, Bahn S, Paabo S, Khaitovich P, Webster MJ (2009) Transcriptome analysis of male-female differences in prefrontal cortical development. Mol Psychiatry 14:558–561

Woodhead GJ, Mutch CA, Olson EC, Chenn A (2006) Cell-autonomous beta-catenin signaling regulates cortical precursor proliferation. J Neurosci 26:12620–12630

Wu Q, Maniatis T (1999) A striking organization of a large family of human neural cadherin-like cell adhesion genes. Cell 97:779–790

Yagi T, Takeichi M (2000) Cadherin superfamily genes: functions, genomic organization, and neurologic diversity. Genes Dev 14:1169–1180

Yamagata K, Andreasson KI, Sugiura H, Maru E, Dominique M, Irie Y, Miki N, Hayashi Y, Yoshioka M, Kaneko K, Kato H, Worley PF (1999) Arcadlin is a neural activity-regulated cadherin involved in long term potentiation. J Biol Chem 274:19473–1979

Yoshida K, Sugano S (1999) Identification of a novel protocadherin gene (PCDH11) on the human XY homology region in Xq21.3. Genomics 62:540–543

Zhang J, Woodhead GJ, Swaminathan SK, Noles SR, McQuinn ER, Pisarek AJ, Stocker AM, Mutch CA, Funatsu N, Chenn A (2010) Cortical neural precursors inhibit their own differentiation via N-cadherin maintenance of beta-catenin signaling. Dev Cell 18:472–479